Design and Manufacturing of a Modular Low-Voltage Multimegawatt High-Speed Solid-Rotor Induction Motor

Emil Kurvinen, Chong Di, Ilya Petrov, Janne Nerg, *Senior Member, IEEE*, Olli Liukkonen, Rafal Piotr Jastrzebski, Daria Kepsu, Pekko Jaatinen, Lassi Aarniovuori, Eerik Sikanen, Juha Pyrhönen, *Senior Member, IEEE*, Jussi Sopanen, *Member, IEEE*, Olli Pyrhönen, Markku Niemelä, and Toni Kangasmäki

***Abstract*—High-speed solid-rotor induction machines (HSIMs) are popular within high-speed (HS) applications because of their high rotor structural integrity and their fairly well-established manufacturing process guaranteeing high quality series products. Designing a new HS electric machine requires a multidisciplinary team to accomplish the machine performance desired. In case of a HS machine design, the components and applied materials often reach their physical limits at the rated operating condition. Therefore, the design process is highly iterative and, thus, a systematic approach has a high potential to reduce the time of the design phase significantly. In this article, a systematic design process is proposed for a modular, multimegawatt (MMW) HSIM with three radial active magnetic bearings. The process includes a traditional multidisciplinary design flow with extra critical aspects of MMW HS machines: manufacturability, bearing system, housing, and operating unit. In addition, the manufactured machine is reported. The proposed systematic design process is described, including several multidisciplinary critical design aspects of HS machinery.**

***Index Terms*—High-speed (HS) induction machine, manufacturing, multidisciplinary, systematic design process.**

Manuscript received November 10, 2020; revised February 3, 2021 and April 9, 2021; accepted May 24, 2021. Date of publication May 26, 2021; date of current version November 19, 2021. This work was supported by the European Regional Council of South Karelia under Grants A73086 and A73066. *(Corresponding author: Emil Kurvinen.)*

Emil Kurvinen, Eerik Sikanen, and Jussi Sopanen are with the Department of Mechanical Engineering, School of Energy Systems, Lappeenranta-Lahti University of Technology LUT,53850 Lappeenranta, Finland (e-mail: emil.kurvinen@lut.fi; eerik.sikanen@lut.fi; jussi.sopanen@lut.fi).

Ilya Petrov, Olli Liukkonen, Rafal Piotr Jastrzebski, Daria Kepsu, Pekko Jaatinen, Lassi Aarniovuori, Juha Pyrhönen, Olli Pyrhönen, Markku Niemelä, and Toni Kangasmäki are with the Department of Electrical Engineering, School of Energy Systems, Lappeenranta-Lahti University of Technology LUT, 53850 Lappeenranta, Finland (e-mail: ilya.petrov@lut.fi; olli.liukkonen@lut.fi; rafal.jastrzebski@lut.fi; Daria.Kepsu@lut.fi; pekko.jaatinen@lut.fi; Lassi.Aarniovuori@lut.fi; juha.pyrhonen@lut.fi; olli.pyrhonen@lut.fi; markku.niemela@lut.fi; toni.kangasmaki@lut.fi).

Chong Di is with the School of Electrical Engineering and Automation, Hefei University of Technology, Hefei 230009, China, and also with the Department of Electrical Engineering, School of Energy Systems, Lappeenranta-Lahti University of Technology LUT, 53850 Lappeenranta, Finland (e-mail: chong.di@lut.fi).

Janne Nerg is with the LUT Energy, Lappeenranta-Lahti University of Technology, 53851 Lappeenranta, Finland (e-mail: janne.nerg@lut.fi).

Color versions of one or more figures in this article are available at https://doi.org/10.1109/TIA.2021.3084137.

Digital Object Identifier 10.1109/TIA.2021.3084137

I. Introduction

HIGH-SPEED (HS) machines can be used in traditional HS applications where a step-up or step-down gear system has been used. There is a billion-dollar market in HS gears indicating that there should be a lot of room for direct HS drive systems [1]. These gears enable the use of normal industrial motors or generators together with a HS flow machine—a compressor or a turbine. Compressors make up for more than 50% of the market volume of HS applications. The latest boom related to HS applications are large heat pumps [2]. Gears represent the traditional case in many other high-speed applications such as, e.g., in microturbine systems. Gears, however, occupy lots of space and need a massive lubrication-oil system. In a case example of a 2 MW step-up gear, a 10 m^3 oil tank is needed and it needs to be located one storey below the gear itself resulting in an expensive and environmentally harsh infrastructure. The no-load friction power of the gear increases with the operating speed and can lead to a significant share of losses at the rated motor speed. A direct HS drive system with active magnetic bearings (AMB), therefore, provides a wide operation speed range with a less complex shaft arrangement and with high efficiency. HS electric machines are capable of achieving a high-power density and can, therefore, be made in a compact and material-efficient form. The machines which have a peripheral speed over 100 m/s are typically considered to be HS machines [3]. Compact form is an attractive feature in different industry sectors and especially in the process industry, transportation, and aerospace. The high power and compact structure leads to design challenges for electrical, mechanical and thermal design, as the machine should have a high efficiency, its structural integrity needs to be ensured and the heat generated by different motor components needs to be dissipated or transferred effectively [4]. The traditional induction machine design approaches do not yield anticipated results for HS machines, and thus, new systematic design approaches are required [5]. An induction motor can have different topologies based on mechanical structure, having a tradeoff between the ease of manufacturability and efficiency. However, in megawatt range the tradeoff is not very significant [6]. Establishing a systematic design process for a HS induction machine allows accomplishment of more tailored designs and eventually

higher efficiency machines. In general, HS machines are customized and designed for a specific case and this prevents mass production of HS machines, potentially applicable in different applications. One approach to ensure suitability to a wider spectrum of cases with different speeds and impellers while ensuring subcritical operation over the whole speed range, is to utilize a modular three-radial-bearing configuration. The additional bearing enables utilization of the machine in different applications with a range of acceptable impeller and coupling sizes, based on the required load capacity [7]. In the literature, the design processes of high-speed induction machines (HSIM) are proposed. However, their coverage is limited. Arkkio *et al.* [8] proposed a flow chart of a HS application design for the HSIM and HS PM machine, but their design process did not include auxiliary parts of the machine such as housing, bearings, and actual operating units (impellers), i.e., the dynamics of the complete machine were not included. Ranft [9] proposed a mechanical design of an HSIM rotor, however, the thermal analysis was not considered. A few design processes are proposed for HS PM machines, such as the one by Kolondzovski *et al.* [10] and Uzhegov *et al.* [4]. Uzhegov *et al.* [4] proposed for low power HS permanent magnet synchronous machine with the tooth coil winding and cylindrical magnet a multidisciplinary systematic design process. In this article, solely the design aspects were considered and, e.g., manufacturing was omitted. In addition,in these machines the rotor diameter is less than 0.05 m and the mass of the rotor is less than 10 kg. This can be considered a traditional HS design process. However, in the case of a megawatt range solid-rotor induction machine, where the rotor diameter is more than 0.2 m and the mass of the rotor is in hundreds of kilograms, the manufacturability, winding assembly development, bearing system, housing, and operating unit bring additional constraints, which are not included in the systematic design process proposed by Uzhegov *et al.* [4]. Smirnov *et al.* [11] proposed optimization for HSIM for electric machines and active magnetic bearing, but they omitted the thermal analyses in their study. Ismagilov *et al.* [12] proposed a multidisciplinary design process for ultra-HS electric machines. However, they did not consider the manufacturability and housing in the design process. The scientific novelty of this study is in describing the systematic design process for a multimegawatt (MMW) HSIM with a solid-rotor including the multidisciplinary platform with extra critical considerations containing manufacturability, bearing system, cooling design, motor housing dynamics, and operating unit issues. Especially, this article focuses on low-voltage configuration of litz wire winding, which has delta connection with parallel paths but is easily manufacturable despite directly water-cooled winding is utilized. The manufacturability of the solid rotor becomes a limiting factor as its physical size is large and for achieving better performance characteristics, it should include a copper squirrel cage in the rotor. Mechanical properties of copper and steel differ from each other making manufacturing of a copper-cage rotor challenging. This combined with the high operating temperature (up to 200 °C) creates true manufacturing challenges. As reported in [6], there are different options for rotor constructions; a solid steel rotor with complete squirrel cage copper winding, slitted solid rotor with copper end rings, or a slitted steel rotor without any other features. In addition, a modular bearing design structure requires extra rotor length and thus reduces the critical speeds. In addition, in large machines the housing dynamics are close with excitation at twice the line frequency, which creates dynamical challenges. Also, the stability of the rotor balance during the rotor thermal cycling is crucial, especially when AMBs are applied and should be considered, when manufacturing methods are analyzed.

II. Systematic Design Process of an HSIM

This research summarizes the steps required to design a new MMW HSIM with a solid rotor. Additional features (when compared to a traditional HS design process) of manufacturability, bearing system, housing, and operating unit are proposed within a systematic design [4]. Fig. 1 depicts a systematic design flowchart for HSIM design process from requirements to commissioning.

The design process is highly iterative and is divided into ten different steps as follows.

A. Step 1: Requirements List

When the process parameters are known, the HS electrical machine design starts from the torque and speed (constant or speed range) of the driven unit, which gives the objectives for rotor dynamical performance and active magnetic bearing utilization. Naturally, the voltage level, the converter type (e.g., the number of phases, voltage and current limits) information and efficiency target are needed, before commencing the design. With ultimate efficiency as target, a permanent magnet machine may be the choice. However, the slip-caused losses in a HS induction machine are so low that in many cases this motor type can compete successfully in finding the most techno-economical solution. In the requirements, the desired technical specifications, of the electric machine are defined including, the physical size, weight, noise level, and desired vibration characteristics, which are important factors in industrial applications. In this research, the topology is limited to induction machines. A feasibility study can, then, be conducted, i.e., a literature and industry review to find if there are similar types of machines available and estimates feasibility with analytical calculations. For example, the aimed tangential stress of the electric machine [13], which is also related to the required cooling and, therefore, approximate limiting values are known for specific type of cooling. This allow to design an approximately right size machine where electromagnetic, structural, and dynamical aspects are accounted and, therefore, perform the thermal analysis in a later phase, when the geometry is well established. In addition, the peripheral velocity and the load capacity per unit area of the AMBs [14] can be used as base boundary values.

B. Step 2. Limiting the Rotor Size

In the second step, the mechanical sizing for different sections is studied, i.e., what is the maximum diameter that the rotor can mechanically withstand in the anticipated operating condition

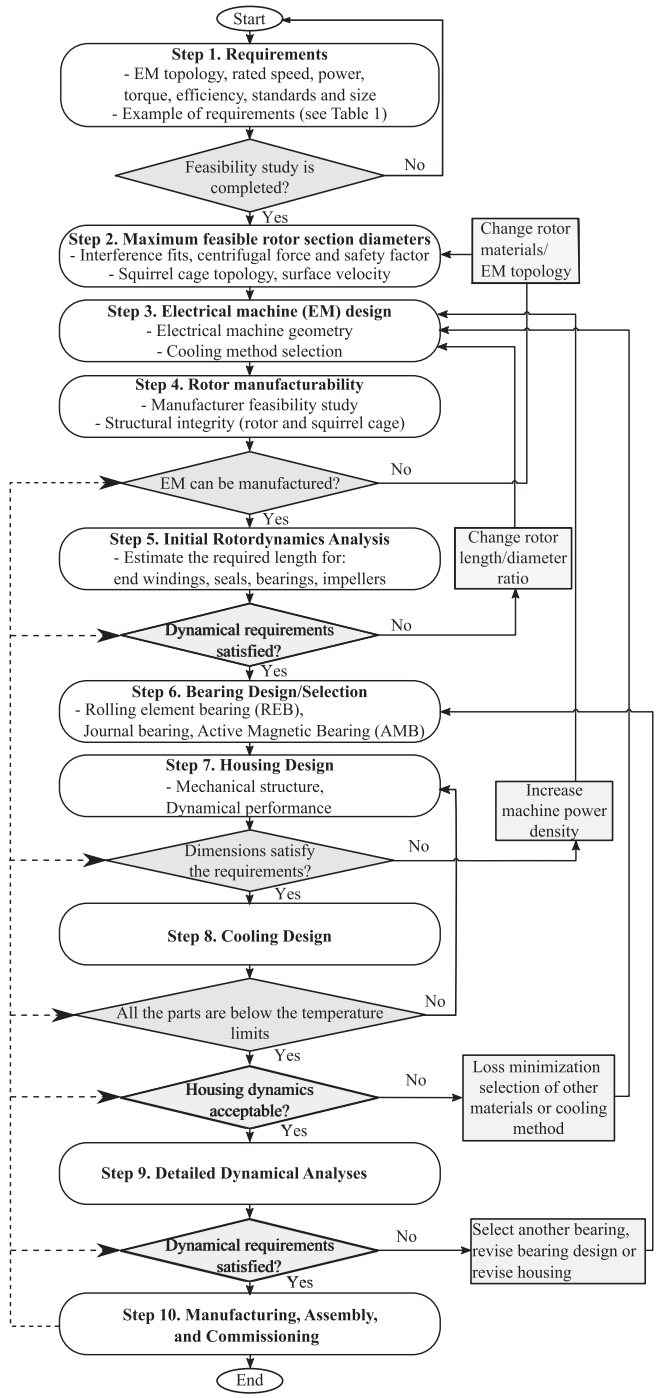

Fig. 1. Flowchart for HSIM design.

with a predefined safety factor. Selection or design of the bearings can be arranged in a similar way, e.g., what size of bearings can handle the speed and load, how for example interference fits should be designed. In the impeller section maximum dimensions can also be tested for different materials. Impeller and other interfaces in the rotor structure must be able to withstand load states at zero-speed and full-speed with and without thermal strain. These four load states form the boundaries for designing the interfaces [8], [15]. Typically, active electromagnetic part has the largest diameter on the main shaft, and is, in practice, limiting the size due to the complex structure of the active part. Understanding the boundaries enables the optimization of the feasibility of the structure. Using the maximum diameter leads to a design where the surface speed is fixed to a maximum and rotor dynamics may have large margins to the first bending mode. However, the air gap friction losses have cubic dependency on the rotor surface speed and, therefore, short stacks with large surface velocity are not running at the best efficiency. In this step, the analytical and FE-based methods can be used.

C. Step 3: Design of the Active Electromagnetic Parts of the Machine

When the maximum mechanically feasible diameter of the rotor is preliminarily defined, then the needed active electromagnetic length of the machine can be calculated with two-dimensional (2-D) FEM-based solutions to reach the aimed torque based on the tangential stress. Here, the torque-producing tangential stress can be approximately defined in advance based on the cooling selection and the rotor topology [13]. The stator structure and stator winding arrangement are designed based on the required efficiency level, available space, and electrical energy supply characteristics [16]. Low-voltage machines and converters of the same power are typically cheaper than high-voltage ones. Therefore, HS machines are designed as low-voltage machines if possible, from the Faraday's law point of view. Stator winding layout has an impact on the machine performance and as a rule, short-pitched winding is preferred to reduce the stator winding harmonics [13].

On the rotor side, as a rule of thumb, we can state that with a HS induction motor the following power level differences with very rough approximation can be used as a guideline in the original design [17]. 1) a machine with a solid slitted rotor (made of steel having similar electromagnetic properties as S355) gives power $P = 1$ p.u. (per unit), 2) if the same rotor is equipped with copper end rings the power can be increased to $P = 1.2$ p.u., i.e., by 20%, 3) if the rotor is equipped with a complete copper cage the power of the machine can be further increased by 20% to $P = 1.44$ p.u. with similar cooling in all the three cases. From this we can immediately find out that if the rotor is going to be just a slitted solid one and the power level 1.44 p.u. is needed, the machine must have a 44% larger rotor, i.e., 13% higher rotor diameter and length are needed, or a squirrel cage must be implemented [17] Moreover, the changes in geometry are tightly connected to the losses and, thus, the actually gained performance will vary. In case of copper-coated solid rotor [18] reliable coating (to withstand high mechanical stresses) involves quite complex and expensive manufacturing processes, such as explosion welding, HIPping or vacuum brazing. Moreover, there is a lack of detailed information about mechanical stiffness for such a construction in HS IMs. Therefore, copper coating was considered out of scope for this article. In addition, smooth rotors were not considered due their poor torque capacity.

D. Step 4: Rotor Manufacturing Feasibility Study

In the fourth step, the electric machine active part manufacturability and final structural integrity need to be verified, this

might require prototyping to verify with the manufacturers. This part is especially important in the case of a full squirrel-cage rotor, the cage should withstand the anticipated loads and operating temperatures and it should by no means harm the rotor balancing during operation. Manufacturing of a large rotor and joining or designing the structure so that different materials (e.g., copper squirrel cage) remain in balance, and rotor integrity in HS operation and thermal cycling require high precision and know-how manufacturing methods and tolerances. In these types of machines brazing and hot isostatic pressing are potential methods to join separate parts. In many cases, however, the rotor cage is arranged in such a way that it may freely move inside the rotor structure to avoid stresses caused by different thermal expansion coefficients of the materials. If the structural integrity cannot be ensured, different materials or EM topology need to be studied.

E. Step 5: Initial Rotordynamic Analysis

In the fifth step, the initial rotordynamic analysis is conducted for the complete rotor using simplified rotor (based on Timoshenko beam element) and bearing models [19], [20]. For example, the estimated spaces and sizes for the end windings, seals, bearings, and in modular configuration the additional radial bearing and impellers are studied. The AMB dimensions and force capacity are designed and cosimulated with different rotor layout options while taking into account additional mass and balancing requirement, and changes in rotordynamics behavior. Often, in case of an AMB-supported machine, the housing and foundation models can be neglected in the initial rotordynamics model. In such a case, the preliminary housing dynamics are studied using estimated foundation stiffness properties. This way, the rotor nominal modes can be calculated and compared to the required operational speed range. If the rotordynamics analysis results are not satisfactory, the EM design needs to be refined, e.g., the length to diameter ratio needs to be decreased. Added length of a machine decreases the rotor critical speeds, and thus, becomes typically, a limiting factor in HS machines [9].

F. Step 6. Bearing Selection

In the sixth step, the bearing design is performed with the given rotor dynamic's space requirements defined in the earlier step. For a machine oriented horizontally, and low-speed operation, the nominal force capacity of radial AMBs is about 4–8 times the gravity force. Additionally, a comfortable lift off force capacity from the safety bearings must be ensured. For example, an E-core 12 pole geometry with flux barriers [7] can provide about 30% higher capacity than the C-core 8-pole classical geometry for the same rotor length and stator outer diameter. ISO 14 839-3 [21] provides recommendations for the evaluation of the stability margins for AMB-supported machinery. The standard suggests that the absolute peak sensitivity is less than 3, for a machine to be designated in safe Zone A. This must be further ensured with closed loop control system responses; and the bearing design has to be reiterated if needed. The axial AMB is designed according to specified axial force and expected bandwidth requirements according to the application. FE-methods are used in the bearing geometry calculation.

G. Step 7. Housing Design

In this step, the housing is designed, i.e., the structure around the rotating part including space for the seals, stators, and the housings for impellers are designed. The main goal of the frame design is to create a lightweight but rigid structure that can be manufactured in a cost-effective way. Depending on the selected bearing arrangement and the initial rotor dynamic analysis, design processes have strict requirements for the support stiffness of the bearing housing. The second design aspect, especially in two-pole machines with a high power rating, comes from twice line frequency excitation ($2f$) that generates force in the radial direction around the stator core [22]. Since the excitation force is generated by the nature of this machine construction, a common approach is to design the housing so that the first global modes, which can be excited by $2f$ excitation are above the required speed range. After this step the size of the full machine is compared to the requirements and if it is, e.g., larger than defined in the requirements the EM power density needs to be increased. However, if the power density of EM cannot be increased any further (e.g., due to cooling or electromagnetic limitations) then the initial size requirements need to be reconsidered. The housing design forms the structure around the rotating part, which enables the analysis of the structure performance as a whole.

H. Step 8: Cooling Design

In the eighth step, cooling design is performed and the temperatures of different sections of the machine are studied. Cooling of an EM defines the achievable maximum power, as losses heat up the active part. The losses can be minimized with design improvements, e.g., by utilizing semimagnetic wedges in slot openings, increasing air gap length. To make machine more tolerant to losses winding insulation class can be raised or cooling made more efficient. In addition, the thermal validation of AMB actuators is important, since it helps to establish the maximum suspension force the bearings can achieve. The force capability of the bearing actuator is limited by the maximum acceptable temperature of the coils. The operation points of the bearing dictated by the angular velocity of the rotor and the value of the suspension force are directly connected to the temperature distribution of the bearing. If no external nonconstant disturbance forces are present, the AMB losses are minimal. The bearing is heated by the electromagnetic losses in the rotor and stator cores, the eddy current losses in the rotor, the Joule losses in the stator windings, and by the warmed-up gas heated by the losses of the machine, including the air gap friction losses. The hot spots of the bearing and the thermal limitation of its coils should be analyzed. Detailed cooling arrangements can be performed with lumped mass model and CFD as the housing is known[23]. The final verification is to study the housing dynamics, especially, to avoid the twice line frequency and possible harmful vibration modes.

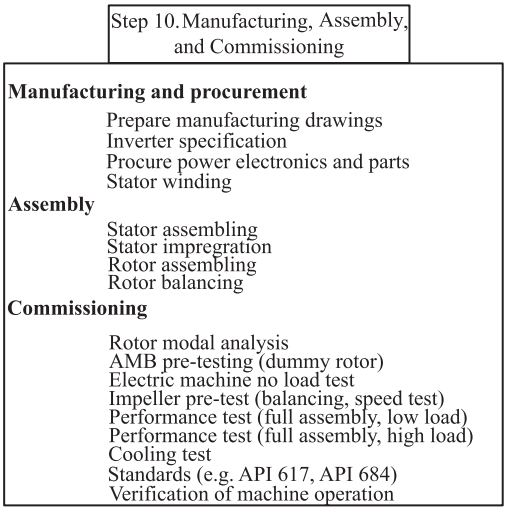

Fig. 2. Final step of the design flowchart (step 10) and actions in it.

TABLE I
TECHNICAL REQUIREMENTS FOR TWO-MEGAWATT MACHINE

Requirement/targets	Requirement	Target
Rated speed	12 000 rpm	-
Maximum speed	16 000 rpm	
Motor type	Induction motor	
Nominal power	2 MW	-
Efficiency at nominal point	>95%	97%
Bearing type	Active magnetic bearing	-
Mechanical safety factor	2.0	-
Stator thermal class	155	130
Rotor thermal class	250	200
Stator cooling method	Direct winding and indirect liquid cooling	Air cooled
Rotor cooling method	Air cooling	-
Rotordynamics	Undercritical	-
IP class	IP20	IP55
Impeller/Coupling mass	15 kg	-
Frame size	500	
Standards	API 617	-
Maintenance period	5 years	10 years

I. Step 9: Detailed Rotordynamics Analysis

The ninth step is to conduct a detailed rotordynamics analysis (with Timoshenko beam element and 3-D FE methods) with the final parameters of the machine. In the case of AMB, the bearing control can be designed to specific position stiffness and, thus, has an influence on the rotordynamics. The actuator and sensor locations with respect to the flexible mode shape node location must be checked. In addition, for large rotors, starting from several hundreds of kg, modal balancing is usually required. Therefore, design of balancing planes needs to be included in the final rotor design. For AMB-supported HS systems, the housing and foundation dynamics can be analyzed using a submodel, and if the subsystem natural frequencies are clearly above the critical speed, often it can be neglected from the rotor-bearing model because of the soft coupling effect between the housing and rotor due to the characteristics of AMBs. In addition, probable low-level high-frequency housing resonances can be suppressed in the bearing controller by utilizing a notch filter. If the dynamics do not satisfy the requirements of the rotor, the bearings and housing designs need to be redone. The rotordynamic analysis requires information of geometries, materials, and manufacturing methods in order to build a model for rotor dynamics analysis.

J. Step 10: Manufacturing, Assembly, and Commissioning

The design will be finalized in this step and at this step the manufacturing of the prototype will be accomplished. During this step the design is critically evaluated and optimized for manufacturing, which includes iteration rounds between designer and manufacturing details (see the dashed connections (see Fig. 1) from Step 10 to decision points). Fig. 2 depicts the action items that are included in the final step. The tenth step is the manufacturing, assembly and commissioning including verification of machine operation.

The first part is the manufacturing and procurement, where ready-made parts, which can be purchased, such as standard parts, e.g., bolts and nuts and power electronics such as inverter operating the electric machine, and AMB related sensing and power electronics are procured. The parts, which will be manufactured need to be prepared for manufacturing, e.g., in sheet metal parts, typically the cutting profile is delivered in DXF-file format. Manual operation manufacturing drawings are needed, and for 3-D manufacturing methods the STEP-file format is typically used. In addition, the stator winding is a multistep process, where discussions with manufacturer require time. The next part is assembling of parts to subassemblies and final assemblies. In this step, the subassemblies are prepared for commissioning to ensure their functional performance, e.g., the short-circuit test for the stator winding and rotor dynamical performance. The final part is commissioning where the subassemblies and finally the full assembly are tested thoroughly. In this step, the final performance of the machine is verified, and its safe operation is tested. This step verifies the design of the HS machine, e.g., the dynamical performance, electrical machine operation, and cooling of the machine.

III. CASE STUDY

With the proposed systematic design flowchart, a multimegawatt HS solid-rotor machine was designed and is being commissioned. Data flows and interfaces between the different engineering disciplines and design process steps are illustrated and discussed. Table I depicts the main requirements for the case study: 2 MW machine.

A. Mechanial Design of the Rotor

Different induction rotor active part designs were conducted [6]. According to preliminary analysis, machine dimensions were selected so that the rotor surface rated speed is 167 m/s, which locates the machine in the lower end of HS machinery leaving a margin for higher speeds. A solid rotor construction is preferred for this kind of application to force the first rotor bending mode above the operational speed range. For this prototype machine, the solid-slitted-rotor design was selected for optimal electro-mechanical design. Therefore, the

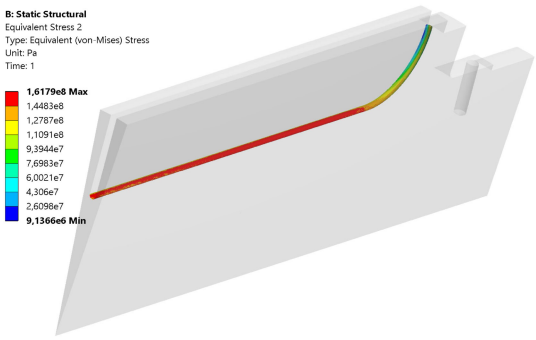

Fig. 3. Stress results of the slit bottom geometry under 12 000 r/min. All the values are well below acceptable stresses when using S355 rotor core material.

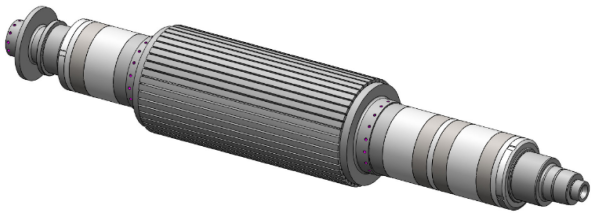

Fig. 4. Design of the rotor construction. Axially slitted solid rotor and three radial AMBs and one axial AMB.

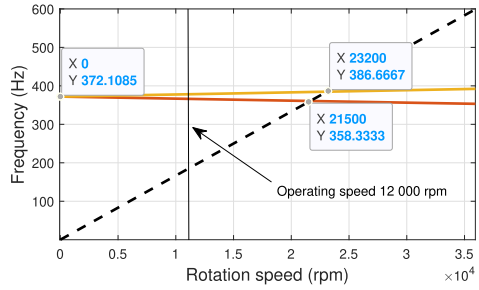

Fig. 5. Campbell diagram of MMW rotor without attachments. The first critical speeds of the rotor are well beyond the operating speed.

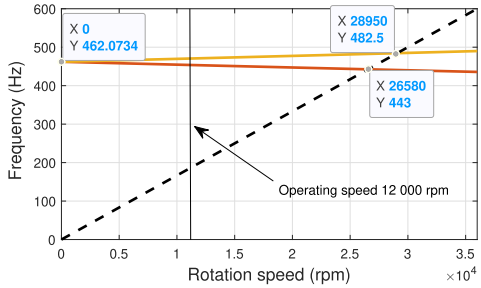

Fig. 6. Campbell diagram of MMW rotor with shaft coupling flange attached to the drive-end.

anticipated power of the prototype is compromised and the actual output capacity is 1.4–1.5 MW, as discussed in Step 3. From the electromagnetic performance point of view, deep slits are preferred. However, a compromise must be done to maintain the mechanical integrity of the rotor. In case of a slitted rotor, the number of slits, width, depth, and the slit bottom geometry are crucial for a successful design [24]. Various slit bottom shapes were studied and the most efficient solution was found to be a semicircle. Fig. 3 shows the stress results of the slit bottom geometry under 12 000 r/min centrifugal load. If the stress levels at the bottom of the slit exceed the material yield strength, a life-time analysis should be conducted, as shown in [25].

The layout of the MMW rotor is depicted in Fig. 4. The nondrive-end is equipped with radial AMB and sensor lamination stacks with detachable axial AMB disk. The drive-end has a double radial bearing and sensor lamination stacks shrink-fitted on the shaft. Two balancing planes for adding balancing screws are located at both sides of the active rotor part. The shaft end at drive-end is equipped with universal conical interface for shrink-fitting an impeller or a mechanical coupling for another machine. The conical sleeve is featured with pressurized oil removal system for shrink-fit interface.

Rotordynamic analysis was made using linearized AMB model for modal domain analysis. For the Campbell diagram, the bearing stiffness and damping were approximated as $5{\cdot}10^6$ N/m and 125 Ns/m. The approximations used are valid for damped eigenvalue analysis since minor shifting in the values does not affect the damped eigenfrequencies. The solved Campbell diagram with different rotor configurations are shown in Figs. 5 and 6. Fig. 5 represents the MMW design rotor critical speeds (forward whirling (FW) frequency of 482.5 Hz and backward whirling (BW) mode of 443 Hz) without any attachments, whereas in Fig. 6, a shaft coupling flange (8.2 kg) is attached to the drive-end of the MMW rotor decreasing the FW to 386.7 Hz and BW to 358.3 Hz.

In addition, the mechanical design of the rotor includes design of shrink-fits (e.g., in AMB laminations), combined thermal loads from EM and AMB's, i.e., thermal cycling.

B. *Electromagnetic Design*

The electromagnetic design of this 2-pole, 660 V, 2 MW, 12000 r/min HS IM is finalized in this section. Fig. 7 shows the finalized 2-D view of the HS IM studied in this article. The electromagnetic design is calculated with time-stepping finite element method. The supply is a pure sinusoidal voltage waveform. It can be seen in the figure that the stator yoke dimension is designed to be large enough to maintain lower flux density within the core for achieving lower core losses and to avoid the two-pole-design-related problem of the twice line frequency in the stator core [22]. Because of the thicker yoke, nominal modes with elliptical mode shape are occurring above twice line frequency excitation. The high yoke also provides more radial space for the end windings of the stator. There are 36 stator slots, which is the minimum number of the slots to ensure that the double-layer short-pitch winding can be used (to mitigate the winding harmonics) for the predefined speed, voltage level, and overall dimensional requirements. Besides, the semimagnetic wedge, as shown in Fig. 7(a), is also utilized on the top of the slot to suppress the slot harmonics. As a result, a smoother air-gap flux density can be obtained, and solid rotor losses can be reduced [26].

Direct-liquid-cooling where the cooling liquid passes through a stainless steel tube inside the winding is applied in the HSIM as

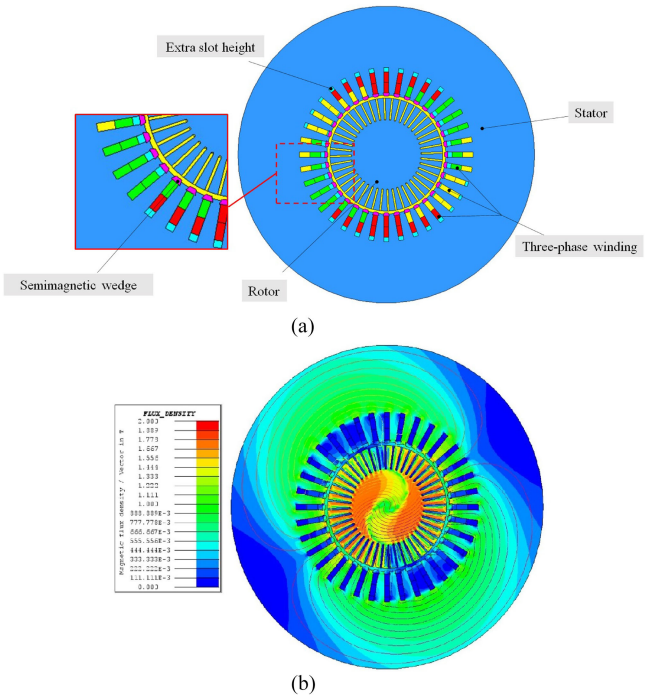

Fig. 7. Finalized geometry of the HS IM and flux density distribution in the domain. (a) Finalized 2-D model of the HS IM. (b) Flux density distribution at the nominal load.

one of the most effective ways for dissipating the heat both from the winding and also the lamination stack made of M270-35 A [27], [28]. However, it limits the options for winding types and arrangement, i.e., Litz wire strands wrapped around steel tubing are utilized, which brings extra challenges in the winding work. To solve this problem, an asymmetric winding is proposed along with the specific winding positioning within the slots, as shown in Fig. 7 [29]. Meanwhile, this asymmetrical winding can bring some current unbalance under load, because different phases have different number of conductors located in the top and bottom of the slots. This phenomenon is fixed by introducing some extra slot height and adjusting the position of the conductors within the stator slots [30].

On the rotor side, a solid rotor made from S355 steel with 44 slits are presented in Fig. 7(a). The rotor dimensions are the optimal results based on the iterative mechanical and electromagnetic design sequence, which guarantee the aimed efficiency and robustness of the machine [24]. The rotor slit depth is about 37% of the rotor radius, which is a comprise between the electromagnetic and mechanical performances. The flux lines shown in Fig. 7(b) verify that the designed rotor achieves a reasonable penetration of the stator flux (or air-gap flux) to the rotor core. This fundamental flux penetration depth affects the overall power factor and efficiency of the induction motor. More details about the electromagnetic design of this machine are shown in [24]. Table II lists the simulated performance characteristics of the machine at the rated load with squirrel caged rotor.

As one can see, the stator winding losses are low compared to the stator iron losses and, especially, the rotor losses. Because of this one might criticize the usage of stator direct liquid cooling and consider it unnecessary. However, this method guarantees low stator winding temperature, especially the end winding temperature where the cooling difficulties are typically imminent. The winding cooling also helps in cooling of the stator teeth and part of the yoke. As the yoke thickness is high a liquid jacket is realized outside the yoke finalizing efficient stator cooling—it is now cooled both on the inner and outer surfaces. The rotor cooling is a challenge and a strong air flow is arranged via both ends of the machine and the flow then escapes from the middle of the stator while it is built of two substacks. The machine protection class is naturally IP20 and if IP55 is needed, a heat exchanger must be attached to the system cooling of the rotor cooling air.

TABLE II
MAIN PERFORMANCES OF THE HS IM

Parameter	Value
Rated power, (kW)	2000
Rated voltage, (Vrms)	660
Rated frequency, (Hz)	200
Synchronous speed, (r/min)	12000
Rated operating speed , (r/min)	11934
Winding connection	Delta
Per-unit slip at the rated load	0.0055
Rated torque, (Nm)	1618
Rated current, (Arms)	2638
Power factor	0.70
Stator copper losses, (kW)	5.11
Solid rotor eddy current losses, (kW)	27.0
Stator core losses, (kW)	17.0
Mechanical losses, (kW)	10.0
Extra losses (added for safety reason, potentially caused by high frequency time harmonics), (kW)	10.0 (0.5%)
Efficiency, (%)	96.5

C. Magnetic Bearing Design

The size and the material of the bearing are decided keeping mechanical limitations in mind. The design of the magnetic bearing is based on the required suspension force capacity. The maximum force of the bearing is decided based on the position of the rotor in the center and the maximum coil current. The force produced by the bearing should on average be assumed to be 90–100% of the maximum force. The definition of the air gap, mechanical gap, average and maximum force, flux saturation, force slew rate, shaft radius, the iron ratio of the total circumferential length and the length employed by the pole, and maximum current density are the objectives of the design of a magnetic bearing providing suspension in desired direction. Different types of active magnetic bearings can be designed, i.e., classical magnetic bearings or E-core magnetic bearings. The machine's three bearing topology design is depicted in Jastrzebski *et al.* [7]. The AMB designs dimensioning, frequency responses and closed loop simulations with virtual prototype were shown in [7]. However, because of manufacturing problems, the number of effective turns has been reduced in radial AMB from 98 to 88 and in the axial AMB from 84 to 71. To compensate for the force capacity, the peak current has been

Fig. 8. Manufactured stator of E-core 12-pole radial AMB with flux barriers before the windings are installed.

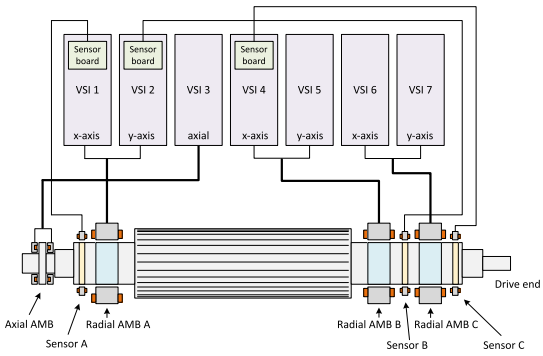

Fig. 9. Block diagram of the control electronics setup. Each VFC is controlling one axis.

increased from 16 A to 21 A compared to the initial design. Fig. 8 shows the manufactured radial AMB stator.

Control electronics is built using commercial voltage source inverters (VSI) to regulate AMB currents. The overall block diagram of this setup is shown in Fig. 9. Selection of the VSIs are based on the current requirement in the AMBs. VSIs are equipped with a custom FPGA board where the inner current controller is implemented. Input port for the separate position sensor electronics is also included. The position sensors used are inductive type that measure the rotor movement in three dimensions. Upper level position controller is implemented in the Beckhoff industrial PC, which is communicating with the VSIs via EtherCAT fieldbus.

D. Thermal Analysis

A transient lumped parameter thermal model comprising of 31 nodes was employed in the thermal analysis of the designed HS induction machine. The cooling is realized by combining direct water cooling in stator windings and in stator housing with conventional forced air cooling for the rotor and AMB's. In the thermal analysis, the losses from electromagnetic design were utilized as heat sources together with the gas friction losses. The ambient temperature was 40 °C and the same value was used as inlet temperature for water and gas. Cooling air was blown to the machine interior from both ends and the air exit was via radial cooling channel. The temperature at stator windings, stator teeth, stator yoke, and rotor surface as a function of time is given in Fig. 10.

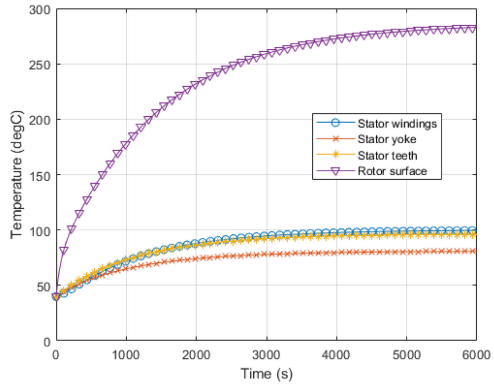

Fig. 10. Calculated temperature at stator windings, stator teeth, stator yoke, and rotor surface as a function of time at nominal speed and nominal power operation.

E. Manufacturing

In the manufacturing phase the final design is critically evaluated. The manufacturability and availability of the individual components is assessed, and the assembly operation are planned in detail. During this step, the design is updated, for example based on the material availability and supplier's comments and chosen manufacturing methods. The selected EM topology naturally affects the rotor manufacturing methods. For example, a slitted rotor can be machined; a slitted rotor with copper end-rings can be machined and then copper end-rings vacuum brazed to the rotor or can be welded using electron beam welding or hot isostatic pressing can be used to join the parts; a copper coat can be welded on the rotor via explosion welding whereas a smooth rotor can be machined. Large components require special attention, for example the frame with shaft height 500 mm, when manufactured by casting with tight tolerances. Manufacturing drawings are prepared based on the final 3-D geometry. During this step, the parts are divided into subassemblies based on the anticipated manufacturing methods, e.g., made from sheet metal, casted, or machined parts. In addition, during this step the procurement of power electronics are done. Components that differ from the conventional electrical machines such as winding arrangement, stator liquid cooling jacket, or stator geometry with skewing require testing and prototyping in the machinery workshop as well.

F. Assembling

The assembling follows typical assembly procedures of an electric machine, where the process starts from rotor and verification of its dimensions and properties. Following is a stator verification as an individual component. The next step is to mount the stator in the housing. Following the end shields installation and assembling the full machine. The final step is to make the required electrical connections. In the assembling step, the verification of subassemblies and their fittings as a whole is performed and checked so that the tolerances are

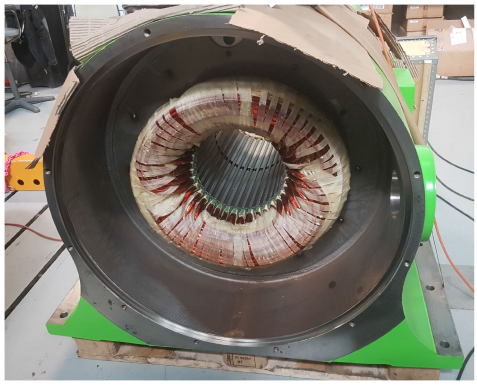

Fig. 11. Manufactured prototype stator.

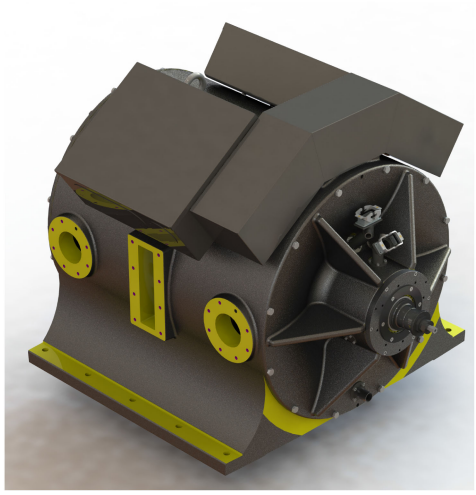

Fig. 12. Designed MMW machine

within the limits. For example, out of roundness parts can lead to alignment errors, which then in the HS operation can be seen as a high vibration amplitude due to magnification per revolution response. Fig. 11 depicts the stator manufactured for the prototype machine and Fig. 12 the designed machine.

G. Commissioning

In the commissioning, the steps depicted in Fig. 2 are taken to ensure safe operation and verified behavior. Commissioning is made in parallel to the assembling step, as the individual subassemblies can be tested individually. For example, structural dynamical verifications are made for both the rotor and the housing. Both structures are measured using a scanning laser vibrometer to identify the mode shapes, frequencies, and modal damping ratios. In case of rotor experimental analysis, the node locations of the lowest flexible bending modes are also identified, to verify that they are not at the sensor locations, which would lead to poor performance of the AMB's. The housing vibration identification is performed without installing the rotor. The identified mode frequencies and damping ratios are used for updating the finite element models of both rotor and housing. Fig. 13 shows the rotor experimental measurement setup.

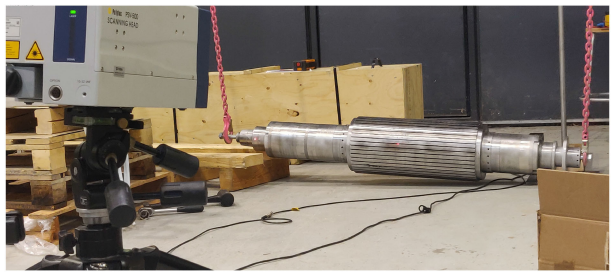

Fig. 13. Rotor during experimental modal analysis.

TABLE III
IDENTIFIED ROTOR FLEXIBLE MODE PROPERTIES

Mode	Frequency	Damping
1. Bending	488.2 Hz	0.9%
2. Bending	893.0 Hz	0.3%
3. Bending	1410.8 Hz	1.4%

The rotor identified mode frequencies and damping ratios for the lowest flexible modes are presented in Table III. Similarly, the housing lowest flexible mode shapes, frequencies, and damping ratios were identified. The updated housing finite element model is used for the AMB controller synthesis. After the rotor installation the commissioning of sensors and actuators is performed. Channel directions, sensor gains and offsets are determined. After that, identification of the AMB-rotor system with AMB actuators and sensors is performed. If required, the plant model is updated while the housing mechanical design is stiffened; sensor and actuator mechanical integration is improved. Model-based centralized controllers are resynthesized for optimal performance.

The commissioning step is especially important in HS applications as the design and manufacturing can include several critical engineering fields (e.g., electromagnetic, rotor dynamics, mechanical stresses, AMBs, and thermal) and in the assembled machine, each individual component should be functional to achieve the overall performance.

IV. DISCUSSION

The design process of a HS machine requires a multidisciplinary research team to accomplish a feasible design, which can be manufactured and assembled at a high precision. Systematic approach enables better planning and clarifies the individual designer tasks at hand and how the task relates to other designer tasks. A systematic design process can lead to multiple feasible solutions, and it should be noted that additional parameters, such as the mass of the rotor could be optimized as well to enhance the operational performance. Structural stress and rotordynamic analyses were performed alongside each other for the MMW rotor design. An electromechanically optimized structure for the rotor active part was selected to be a slitted design due to its simplicity and good thermal endurance. However, this selection compromises the maximum power that the motor can produce and to accomplish the full anticipated capacity of 2 MW, full squirrel cage rotor needs to be developed. During the manufacturing step, changes to the design are made, and thus, the design

of the final version needs to be assessed. Based on the experiences gathered from MMW prototype machine manufacturing, focus must be placed on components made by casting. Another time consuming and multiple iterations requiring component is the stator winding. The winding construction must be modeled and pretested before the manufacturing drawings of the main components are fixed. From the robustness of the closed-loop control system perspective the radial AMB next to axial AMB disc should be resized to achieve a 20–30% higher load capacity, as it is limiting the output sensitivity peak.

V. Conclusion

The number of HS machines in different applications are rising. They are used, for example in direct drive solutions such as compressors and turbines. The developments in the material and manufacturing technology enable new electrical machine design with higher performance, increased speeds, and lower weight. More accurate design methods are needed to take advantage of aforementioned technologies. The proposed design process was used to create a high-performance HS (12 000 r/min) 2 MW electrical machine with a wide application scope. The selected direct water cooling in the winding provides a superior cooling performance for the stator despite the high temperature experienced by the solid rotor. To verify the mechanical usability of the designed rotor in a HS machine system equipped with AMBs, the natural frequencies of the assembled rotor were verified. The proposed systematic design process streamlines the highly iterative HS electric machine design process. In further studies, additional optimization loops and improved automatization within the individual steps will be developed. In addition, different HS machine topologies, e.g., bearingless machines are of interest.

References

[1] StrategyR, "Industrial gearbox - global market trajectory & analytics," Global Industry Analyst Inc., San Jose, California, United States, Report I.D. 4805819, Sep. 2020.

[2] Uniturbo-50FY, *Centrifugal Compressor for Large Scale Refrigeration Plants and Heat Pumps*, 2017. [Online]. Available: https://www.friotherm.com/wp-content/uploads/2017/12/turbo50fy_uk_g008.pdf

[3] E. Kurvinen, "Design and simulation of high-speed rotating electrical machinery," Ph.D. dissertation, Lappeenranta University of Technology, Lappeenranta, Finland, 2016.

[4] N. Uzhegov, E. Kurvinen, J. Nerg, J. Pyrhönen, J. T. Sopanen, and S. Shirinskii, "Multidisciplinary design process of a 6-slot 2-pole high-speed permanent-magnet synchronous machine," *IEEE Trans. Ind. Electron.*, vol. 63, no. 2, pp. 784–795, Feb. 2016.

[5] J. Barta, N. Uzhegov, P. Losak, C. Ondrusek, M. Mach, and J. Pyrhönen, "Squirrel-cage rotor design and manufacturing for high-speed applications," *IEEE Trans. Ind. Electron.*, vol. 66, no. 9, pp. 6768–6778, Sep. 2019.

[6] E. Kurvinen, C. Di, I. Petrov, R. P. Jastrzebski, D. Kepsu, and J. Pyrhönen, "Comparison of the performance of different asynchronous solid-rotor constructions in a megawatt-range high-speed induction motor," in *Proc. IEEE Int. Elect. Mach. Drives Conf.*, 2019, pp. 820–825.

[7] R. P. Jastrzebski, E. Kurvinen, and O. Pyrhönen, "Design, modelling and control of MIMO AMB system with 3 radial bearing planes for megawatt-range high-speed rotor," in *Proc. IEEE Int. Elect. Mach. Drives Conf.*, 2019, pp. 805–811.

[8] A. Arkkio, T. Jokinen, and E. Lantto, "Induction and permanent-magnet synchronous machines for high-speed applications," in *Proc. Int. Conf. Elect. Mach. Syst.*, 2005, vol. 2, pp. 871–876

[9] C. J. G. Ranft, "Mechanical design and manufacturing of a high speed induction machine rotor," Ph.D. dissertation, North-West University, Potchefstroom, South Africa, 2010.

[10] Z. Kolondzovski, A. Arkkio, J. Larjola, and P. Sallinen, "Power limits of high-speed permanent-magnet electrical machines for compressor applications," *IEEE Trans. Energy Convers.*, vol. 26, no. 1, pp. 73–82, Mar. 2011.

[11] A. Smirnov, N. Uzhegov, T. Sillanpää, J. Pyrhönen, and O. Pyrhönen, "High-speed electrical machine with active magnetic bearing system optimization," *IEEE Trans. Ind. Electron.*, vol. 64, no. 12, pp. 9876–9885, Dec. 2017.

[12] F. R. Ismagilov, N. Uzhegov, V. E. Vavilov, V. I. Bekuzin, and V. V. Ayguzina, "Multidisciplinary design of ultra-high-speed electrical machines," *IEEE Trans. Energy Convers.*, vol. 33, no. 3, pp. 1203–1212, Sep. 2018.

[13] J. Pyrhönen, T. Jokinen, and V. Hrabovcova, *Design of Rotating Electrical Machines*. Hoboken, NJ, USA: Wiley, 2013.

[14] A. Tonoli, A. Bonfitto, M. Silvagni, L. D. Suarez, and F. Beltran-Carbajal, "Rotors on active magnetic bearings: Modeling and control techniques," in *Advances in Vibration Engineering and Structural Dynamics*. Rijeka, Croatia: InTech, 2012, pp. 1–3.

[15] R. Larsonneur, "Design and control of active magnetic bearing systems for high speed rotation," Ph.D. dissertation, Swiss Federal Institute of Technology, Zürich, Switzerland, 1990.

[16] N. Fernando, P. Arumugam, and C. Gerada, "Design of a stator for a high-speed turbo-generator with fixed permanent magnet rotor radius and volt-ampere constraints," *IEEE Trans. Energy Convers.*, vol. 33, no. 3, pp. 1311–1320, Sep. 2018.

[17] J. Huppunen, "High-speed solid-rotor induction machine-electromagnetic calculation and design," Ph.D. dissertation, Lappeenranta University of Technology, Lappeenranta, Finland, 2004.

[18] J. F. Gieras and J. Saari, "Performance calculation for a high-speed solid-rotor induction motor," *IEEE Trans. Ind. Electron.*, vol. 59, no. 6, pp. 2689–2700, Jun. 2012.

[19] W. J. Chen, E. J. Gunter *et al.* Introduction to dynamics of rotor-bearing systems, vol. 175. *Victoria, Canada: Trafford*, 2007.

[20] M. I. Friswell, J. E. Penny, S. D. Garvey, and A. W. Lees, *Dynamics of Rotating Machines*. Cambridge, U.K. : Cambridge Univ. Press, 2010.

[21] International Organization for Standardization, "Mechanical vibration . Vibration of rotating machinery equipped with active magnetic bearings — Part 3: Evaluation of stability margin," ISO, Vernier, Geneva, Switzerland, 14839-3:2006, Sep. 2006.

[22] W. R. Finley, M. M. Hodowanec, and W. G. Holter, "An analytical approach to solving motor vibration problems," *IEEE Trans. Ind. Appl.*, vol. 36, no. 5, pp. 1467–1480, Sep./Oct. 2000.

[23] J. Nerg, M. Rilla, and J. Pyrhonen, "Thermal analysis of radial-flux electrical machines with a high power density," *IEEE Trans. Ind. Electron.*, vol. 55, no. 10, pp. 3543–3554, Oct. 2008.

[24] C. Di, "Modeling and analysis of a high-speed solid-rotor induction machine," Ph.D. dissertation, Lappeenranta University of Technology, Lappeenranta, Finland, 2020.

[25] T. Aho, J. Nerg, J. Sopanen, J. Huppunen, and J. Pyrhönen, "Analyzing the effect of the rotor slit depth on the electric and mechanical performance of a solid-rotor induction motor," *Int. Rev. Elect. Eng.*, vol. 1, no. 4, pp. 516–525, 2006.

[26] C. Di, I. Petrov, and J. Pyrhönen, "Modeling and mitigation of rotor eddy-current losses in high-speed solid-rotor induction machines by a virtual permanent magnet harmonic machine," *IEEE Trans. Magn.*, vol. 54, no. 12, pp. 1–12, Dec. 2018.

[27] I. Petrov, P. Lindh, M. Niemelä, E. Scherman, O. Wallmark, and J. Pyrhönen, "Investigation of a direct liquid cooling system in a permanent magnet synchronous machine," *IEEE Trans. Energy Convers.*, vol. 35, no. 2, pp. 808–817, Jun. 2020.

[28] P. M. Lindh, I. Petrov, R. S. Semken, M. Niemelä, J. Pyrhönen, L. Aarniovuori, T. Vaimann, and A. Kallaste, "Direct liquid cooling in low-power electrical machines: Proof-of-concept," *IEEE Trans. Energy Convers.*, vol. 31, no. 4, pp. 1257–1266, Dec. 2016.

[29] J. Pyrhönen, C. Di, and I. Petrov, "An electric machine element, a method for manufacturing the same, and an electric machine," *Finland Pat. FI128 226 A*, 2018.

[30] C. Di, I. Petrov, and J. Pyrhönen, "Design of a high-speed solid-rotor induction machine with an asymmetric winding and suppression of the current unbalance by special coil arrangements," *IEEE Access*, vol. 7, pp. 83 175–83 186, 2019.